


RESEARCH ARTICLE

Interactions of optic radiation lesions with retinal and brain atrophy in early multiple sclerosis

Ting-Yi Lin^{1,2,3} , Claudia Chien^{1,2,3,4}, Joseph Kuchling^{1,2,3,5} , Susanna Asseyer^{1,2,3,6}, Seyedamirhosein Motamedi^{1,2,3,6} , Judith Bellmann-Strobl^{1,2,3,6}, Tanja Schmitz-Hübsch^{1,2,3,6} , Klemens Ruprecht⁵ , Alexander U. Brandt^{1,2,3} , Hanna G. Zimmermann^{1,2,3,6,7,*}  & Friedemann Paul^{1,2,3,5,6,*} 

¹Experimental and Clinical Research Center, a cooperation between the Max Delbrück Center for Molecular Medicine in the Helmholtz Association and the Charité – Universitätsmedizin Berlin, Berlin, Germany

²Charité – Universitätsmedizin Berlin, corporate member of Freie Universität Berlin and Humboldt-Universität zu Berlin, Berlin, Germany

³Max-Delbrück Center for Molecular Medicine in the Helmholtz Association, Berlin, Germany

⁴Department of Psychiatry and Psychotherapy, Charité – Universitätsmedizin Berlin, corporate member of Freie Universität Berlin, Humboldt-Universität zu Berlin, Berlin, Germany

⁵Department of Neurology, Charité – Universitätsmedizin Berlin, corporate member of Freie Universität Berlin and Humboldt-Universität zu Berlin, Berlin, Germany

⁶Neuroscience Clinical Research Center, Charité – Universitätsmedizin Berlin, corporate member of Freie Universität Berlin and Humboldt-Universität zu Berlin, Berlin, Germany

⁷Einstein Center Digital Future, Berlin, Germany

Correspondence

Friedemann Paul, Experimental and Clinical Research Center, Lindenberger Weg 80, Berlin 13125, Germany. Tel: +49 30 450 540 012; Fax: +49 450 539 915; E-mail: friedemann.paul@charite.de

Received: 6 July 2023; Revised: 27 September 2023; Accepted: 15 October 2023

Annals of Clinical and Translational Neurology 2024; 11(1): 45–56

doi: 10.1002/acn3.51931

*These authors contributed equally as senior authors.

Abstract

Objective: Retrograde trans-synaptic neuroaxonal degeneration is considered a key pathological factor of subclinical retinal neuroaxonal damage in multiple sclerosis (MS). We aim to evaluate the longitudinal association of optic radiation (OR) lesion activity with retinal neuroaxonal damage and its role in correlations between retinal and brain atrophy in people with clinically isolated syndrome and early MS (pweMS). **Methods:** Eighty-five pweMS were retrospectively screened from a prospective cohort (Berlin CIS cohort). Participants underwent 3T magnetic resonance imaging (MRI) for OR lesion volume and brain atrophy measurements and optical coherence tomography (OCT) for retinal layer thickness measurements. All pweMS were followed with serial OCT and MRI over a median follow-up of 2.9 (interquartile range: 2.6–3.4) years. Eyes with a history of optic neuritis prior to study enrollment were excluded. Linear mixed models were used to analyze the association of retinal layer thinning with changes in OR lesion volume and brain atrophy. **Results:** Macular ganglion cell-inner plexiform layer (GCIPL) thinning was more pronounced in pweMS with OR lesion volume increase during follow-up compared to those without (Difference: $-0.82 \mu\text{m}$ [95% CI: -1.49 to -0.15], $p = 0.018$). Furthermore, GCIPL thinning correlated with both OR lesion volume increase (β [95% CI] = -0.27 [-0.50 to -0.03], $p = 0.028$) and brain atrophy (β [95% CI] = 0.47 [0.25 to 0.70], $p < 0.001$). Correlations of GCIPL changes with brain atrophy did not differ between pweMS with or without OR lesion increase ($\eta_p^2 = 5.92e^{-7}$, $p = 0.762$). **Interpretation:** Faster GCIPL thinning rate is associated with increased OR lesion load. Our results support the value of GCIPL as a sensitive biomarker reflecting both posterior visual pathway pathology and global brain neurodegeneration.

Introduction

Multiple sclerosis (MS) is an immune-mediated disease of the central nervous system (CNS). The dysregulated immune

system in MS results in CNS inflammation and subsequently leads to neuroaxonal damage and degeneration.¹ The afferent visual pathway is highly susceptible to MS damage, making it a promising region of interest to understand the course of

neuroaxonal degeneration in MS.^{2,3} Each individual component within the visual pathway, including the retina, optic nerves, lateral geniculate nucleus, optic radiation (OR), and primary visual cortex, has been investigated as a possible region to measure disease activity in MS clinical trials.^{3,4}

Frequently occurring inflammation of the optic nerve (optic neuritis [ON]) can lead to progressive retinal ganglion cell (RGC) axonal or neuronal loss.⁵ The damage of RGCs following an episode of ON is well-known, and evidenced by optical coherence tomography (OCT) derived retinal measures.^{6,7} These OCT measures have also been considered biomarkers of disease activity for those without a clinical history of ON.^{6,7} Nevertheless, the exact mechanism of this pathological process remains unclear, where a multitude of hypothetical pathophysiological processes, including subclinical inflammation of the optic nerve and primary retinal MS-related pathology or trans-synaptic neurodegeneration, has been previously discussed as candidate theories.^{8–10}

Recent studies have suggested a retrograde trans-synaptic axonal degeneration hypothesis, which refers to degeneration of neurons in the posterior visual pathway spreading via the synaptic cleft of thalamic lateral geniculate nucleus further up-stream to optic nerve fibers and RGC neurons, as one of the key drivers of subclinical retinal neuroaxonal damage. This hypothesis was supported by a significant correlation between OR white matter MS pathology and retinal thinning both cross-sectionally and longitudinally.^{9,11,12} The findings were found to be mainly driven by inflammatory T2 lesions localized within the OR region. However, this observation has yet to be confirmed in people with clinically isolated syndrome (CIS) or early MS (pweMS).¹³ Further data showing the association of visual pathway injury with increased brain atrophy could also support the idea of using retinal imaging outcomes as complementary measures to magnetic resonance imaging (MRI).^{14–17}

In this study, we explore the longitudinal association of RGC neuroaxonal loss, as evaluated by peri-papillary retinal nerve fiber layer (pRNFL) and macular ganglion cell-inner plexiform layer (GCIPL) thinning, with increased OR lesion load and brain atrophy. We hypothesized that: (1) pweMS with increasing OR lesion volume will display accelerated thinning of pRNFL or GCIPL compared to pweMS with stable OR lesions, (2) higher OR lesion volume is associated with homonymous hemi-macular GCIPL thinning, and (3) the association of brain atrophy and retinal thinning will be detected in pweMS with OR lesion activity.

Methods

Study design

We retrospectively screened pweMS from a longitudinal observational study (Berlin CIS cohort: [ClinicalTrials.gov](https://www.clinicaltrials.gov)

Identifier: NCT01371071) conducted at the NeuroCure Clinical Research Center, Charité – Universitätsmedizin Berlin. All pweMS underwent annual follow-up visits for clinical examination, retinal OCT, and brain MRI scans. The study was approved by the institutional ethics committee of the Charité – Universitätsmedizin Berlin (EA1/182/10) and conducted in accordance with the current applicable version of the Declaration of Helsinki. All participants provided written informed consent. Criteria for inclusion into the analysis were (1) time since first clinical manifestation of less than 2 years at baseline, (2) a confirmed diagnosis of early relapsing–remitting MS (RRMS) according to the 2017 McDonald criteria¹⁸ or a monophasic episode suggestive of CNS inflammatory demyelination not meeting the 2017 McDonald criteria for RRMS, (3) baseline age \geq 18 years, and (4) follow-up duration of at least 2.5 years. PweMS with (1) prior ON in both eyes, (2) refractive errors greater than ± 6 diopters, or (3) a history of other neurological or ophthalmological disorders unrelated to MS affecting the OCT analysis were excluded.

Optical coherence tomography

Retinal OCT was acquired using a Spectralis spectral domain OCT machine (Heidelberg Engineering, Heidelberg, Germany). The GCIPL thickness was calculated from a macular volume scan, and the pRNFL thickness was measured through a peri-papillary ring scan. Scanning protocols and details of the segmentation methods were described previously.^{19,20} All OCT scans were quality controlled following the OSCAR-IB criteria, segmentations of the retinal layers were manually reviewed, and data were reported in accordance with the APOSTEL recommendations.^{21,22} Only eyes without a history of ON prior to study enrollment and no further ON attacks during follow-up were included.

Magnetic resonance imaging (MRI) acquisition

MRI was performed for all participants using two 3T scanners (Tim Trio, Siemens, Erlangen, Germany). The MRI protocol included a 3D T1-weighted (T1w) magnetization prepared rapid acquisition gradient echo (MPRAGE) sequence (TR/TE/TI = 1900/2.55/900 ms, 1 mm isotropic resolution) and a 3D T2-weighted (T2w) fluid-attenuated inversion recovery sequence (FLAIR) (TR/TE/TI = 6000/388/2100 ms, 1 mm isotropic resolution) of the brain.

MRI analysis

For each participant, T2w FLAIR images were co-registered with T1w MPRAGE images, in which each

follow-up MPRAGE was co-registered to the baseline MPRAGE in Montreal Neurological Institute (MNI) space using FMRIB's Linear Image Registration Tool from FMRIB Software Library (FSL version 5.0.9).²³ Whole-brain T2w lesion masks were manually segmented from co-registered FLAIR scans using ITK-SNAP (www.itksnap.org) by two MRI technicians (over 10 years of MS research experience).²⁴ MPRAGE scans were lesion-infilled using FSL lesion filling algorithm²⁵ after extracting white matter whole-brain masks using CAT12 (<https://neurojena.github.io/cat/>). The templates of left and right OR were extracted from the Jülich probabilistic atlas²⁶ provided by FSL with lower thresholds of 20% probability, defined by visual assessment of expert rater, to create a binary mask of both ORs in the standard MNI space. We then used FMRIB's nonlinear image registration tool (FSL-FNIRT) from FSL (version 5.0.9) to nonlinearly register the MNI-152 standard brain to the individual MPRAGE of each subject. Subsequently, we used the resulting warp files to nonlinearly register the binary OR masks from MNI space onto the corresponding T1w MPRAGE to create binary OR masks for each subject's individual T1w MPRAGE. Finally, binary OR atlas masks that were warped to the subject's individual T1w MPRAGE were used to extract OR lesions from whole-brain T2w lesion masks that were already co-registered to T1w MPRAGE for initial lesion segmentation. Lesion counts and volumes were calculated using FSL cluster and fslmaths. Brain atrophy was estimated using the percentage brain volume change (PBVC) calculated at each follow-up visit MPRAGE compared to the previous visit MPRAGE using the SIENA pipeline (FSL version 5.0.9).²⁷

Statistical analysis

We separated the cohort into two groups based on the presence (ORL⁺) or absence (ORL⁻) of new or enlarging OR lesions at the 3-year follow-up. The third-year follow-up for all pweMS fell within the time frame of 2.5 to 3.5 years. Due to the lack of a standard definition for OR lesion enlargement, we considered a 10% volume increase for classification.²⁸ Group comparison of demographics and clinical characteristics at baseline were performed using Student's t-test, chi-squared test or Wilcoxon rank-sum test depending on the distribution of the variables.

Cross-sectional and longitudinal association of OCT measures with OR lesion counts and volume and PBVC were analyzed using linear mixed effect models (LMM) (OR lesion measures or PBVC + age + sex + receiving DMT before study inclusion + disease type as fixed effects with random subject intercepts). OR lesion counts and volume (baseline, annualized change and total change at 3-year follow-up) were log transformed to meet the

normal distribution assumption in parametric analyses. To evaluate the ORL⁺ and ORL⁻ group differences concerning the association between retinal layer thickness changes and PBVC, we further conducted interaction analyses and reported the interaction effect size with partial eta-squared (η_p^2). The results of correlation analyses were reported using the standardized regression coefficient (β) and 95% confidence interval (CI).

In longitudinal analyses, LMM were used to study the group differences in the course of retinal layer thickness changes over time (interaction between time since baseline and group as fixed effects, along with random subject and eye-specific intercepts and time since baseline as random slopes). Data at every follow-up visit were included for this longitudinal analysis.

For all models, the statistical significance was set at *p*-value of less than 0.05. Because our analyses followed predefined hypotheses and only included OCT measures relevant for retinal neuroaxonal degeneration, no correction for multiple comparisons was performed. All statistical analyses were performed in R version 4.2.0 (R packages: lme4, lmerTest, ggpubr, ggplot2, effectsize, and emmeans).²⁹ Continuous variables are presented as either mean with standard deviation (SD) or median with interquartile range (IQR), as applicable.

Results

Cohort characteristics

From 166 pweMS screened, 76 were not followed for more than 2.5 years and five had a history of ON in both eyes (see flow chart in Fig. 1). After screening, 85 pweMS (137 non-ON eyes) with a median follow-up of 2.9 years (IQR: 2.6 to 3.4 years) were eligible for inclusion. Sixty-three (74.1%) participants fulfilled the 2017 McDonald MS diagnostic criteria for relapsing–remitting MS (RRMS)¹⁸; the remaining 22 (25.9%) participants were classified as CIS.

Upon study enrollment, 75 (88.2%) pweMS presented detectable OR lesions, while 10 (11.8%) did not. Over the course of 3-year follow-up, 58 (68.2%) participants showed new or enlarging OR lesions (ORL⁺ group), of which 53 (91.4%) already had OR lesions at baseline. Among the remaining 27 (31.8%) pweMS without new OR lesion activity (ORL⁻ group) after 3 years, 22 (81.5%) had detectable OR lesions at baseline.

Demographic characteristics, including age, sex, time since disease onset, relapse rate, and Expanded Disability Status Scale, did not differ between ORL⁺ and ORL⁻ participants. However, a higher proportion of participants in the ORL⁺ group had received disease-modifying therapies (DMT) before study inclusion. Of the 85 pweMS

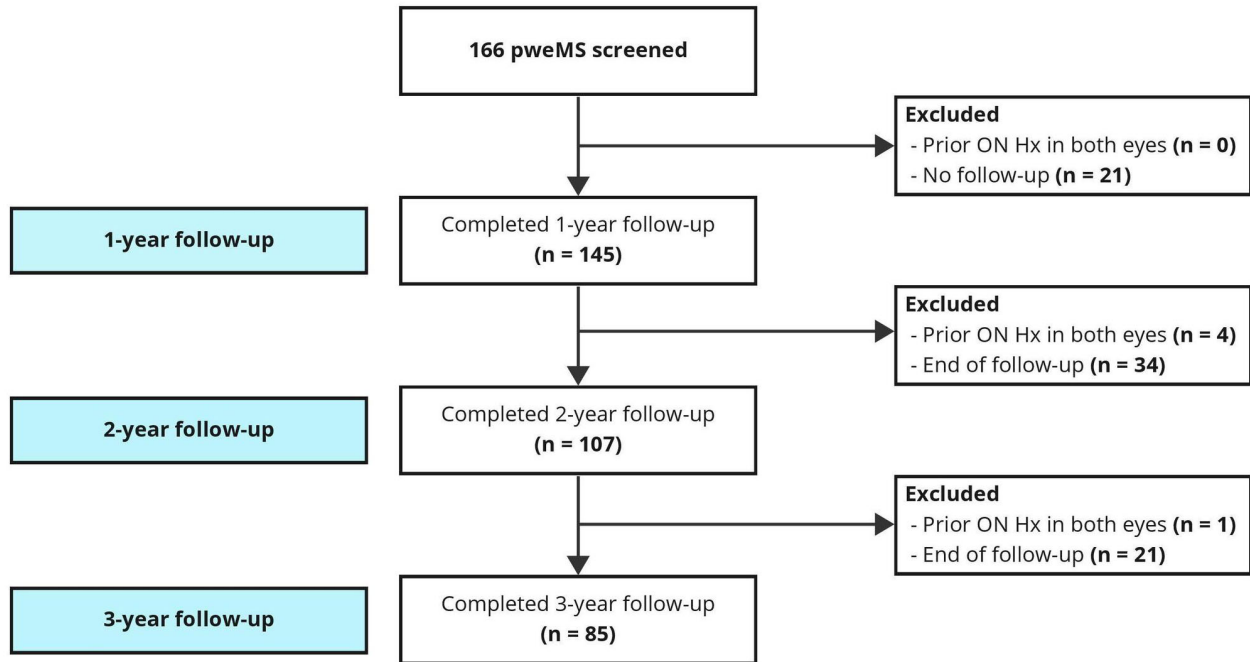


Figure 1. STROBE flow chart. ON, optic neuritis; pweMS, people with early multiple sclerosis.

included, 21 (24.7%) received DMT treatment at baseline. Among them, 12 received DMT only at baseline, one received the same DMT regimen again during the 3-year follow-up, and eight received a second type of DMT (two switched to high efficacy DMTs). Additionally, 32 (37.6%) pweMS received DMT only during follow-up. Among these 32 pweMS, 28 received only one type of DMT, and four received two different types of DMT treatments throughout the study period (two switched to high efficacy DMTs). Nevertheless, there was no significant difference in DMT rates during the study between the two groups ($p = 0.377$). At baseline, compared to the ORL^- group (44 eyes from 27 pweMS), the ORL^+ group (93 eyes from 58 pweMS) showed thinner pRNFL ($-5.53 \mu\text{m}$ [95% CI: -10.21 to -0.85], $p = 0.023$) and, albeit not reaching statistical significance, thinner GCIPL ($-2.68 \mu\text{m}$ [95% CI: -5.45 to 0.10], $p = 0.063$). Additionally, the ORL^+ group also exhibited higher baseline OR lesion count and volume. (Table 1).

Baseline associations of OCT measures with OR lesion volume

At baseline, higher OR lesion volume was associated with both lower GCIPL thickness (β [95% CI] = -0.32 [-0.56 to -0.07], $p = 0.013$) and lower pRNFL thickness (β [95% CI] = -0.28 [-0.50 to -0.05], $p = 0.018$). Similar findings were also observed with OR lesion count

(GCIPL: β [95% CI] = -0.26 [-0.50 to -0.02], $p = 0.033$; pRNFL: β [95% CI] = -0.26 [-0.51 to -0.02], $p = 0.031$). However, there was no significant difference in both GCIPL and pRNFL thickness between participants with detectable OR lesions at baseline ($N = 75$) and those without ($N = 10$) ($p = 0.104$ and $p = 0.075$, respectively). Interaction analyses showed no relevant inter-group difference between those with or without DMT treatment before study inclusion (Table S1).

Longitudinal associations of retinal layer thinning with OR lesion volume change

The rates of retinal layer thinning during follow-up and group comparisons by presence or absence of new or enlarging OR lesions are shown in Table 2 and Figure 2.

Participants in both groups had decreasing GCIPL and pRNFL thickness during follow-up (Table 2). In comparison with the ORL^- group, the eyes from the ORL^+ participants exhibited faster, yet nonsignificant, thinning of the GCIPL ($-0.29 \mu\text{m}/\text{year}$ vs. $-0.12 \mu\text{m}/\text{year}$; annual thinning rate difference: $-0.17 \mu\text{m}/\text{year}$ [95% CI: -0.38 to 0.04], $p = 0.134$) and pRNFL ($-0.52 \mu\text{m}/\text{year}$ vs. $-0.38 \mu\text{m}/\text{year}$; annual thinning rate difference: $-0.13 \mu\text{m}/\text{year}$ [95% CI: -0.77 to 0.52], $p = 0.707$). At 3-year follow-up, the mean GCIPL decrease from baseline was $0.98 \pm 1.42 \mu\text{m}$ in ORL^+ participants compared with

Table 1. Demographics and clinical characteristics of study participants.

	Entire cohort	ORL ⁺	ORL ⁻	ORL ⁺ vs. ORL ⁻ <i>p</i> -value
Participants (<i>N</i>)	85	58	27	–
Eyes (<i>N</i>) ¹	137	93	44	–
Sex, F (%) / M (%)	55 (64.7%) / 30 (35.3%)	37 (63.8%) / 21 (36.2%)	18 (66.7%) / 9 (33.3%)	0.796
Age at baseline (years)	34.3 (8.7)	35.0 (8.5)	32.9 (9.0)	0.347
Mean (SD)				
Disease duration at baseline (months)	4.5 [2.9–5.7]	4.6 [3.0–5.7]	4.4 [2.9–5.6]	0.828
Median [IQR]				
Previous DMT, <i>N</i> (%)				
IFN	6 (7.1%)	3 (5.2%)	3 (11.1%)	0.031
GA	11 (12.9%)	11 (19.0%)	0 (0.0%)	
DMF	3 (3.5%)	3 (5.2%)	0 (0.0%)	
NT	1 (1.2%)	1 (1.7%)	0 (0.0%)	
No treatment	64 (75.3%)	40 (69.0%)	24 (88.9%)	
Ever treated with DMT, <i>N</i> (%)				
Yes	53 (62.4%)	38 (65.5%)	15 (55.5%)	0.377
No	32 (37.6%)	20 (34.5%)	12 (44.5%)	
Follow-up duration (years)	2.8 [2.6–3.5]	2.8 [2.7–3.5]	2.8 [2.5–3.0]	0.248
Median [IQR]				
Presence of relapse during follow-up, <i>N</i> (%)	34 (40.0%)	23 (39.7%)	11 (40.7%)	0.924
EDSS at baseline	1.5 [1.0–2.0]	1.5 [1.0–2.0]	1.5 [1.0–2.0]	0.882
Median [IQR]				
Disease Subtype, <i>N</i> (%)				
CIS	22 (25.9%)	13 (22.4%)	9 (33.3%)	0.285
RRMS	63 (74.1%)	45 (77.6%)	18 (66.7%)	
OR lesion count at baseline (<i>N</i>)	3 [1–7]	5 [2–9]	2 [0–4]	<0.001
Median [IQR]				
OR lesion volume at baseline (mm ³)	144 [39–442]	201.5 [103–508.75]	35 [0–206]	<0.001
Median [IQR]				
pRNFL thickness at baseline (μm)	101.0 (10.1)	98.9 (9.7)	105.2 (10.0)	0.023
Mean (SD)				
GCIPL thickness at baseline (μm)	71.3 (5.9)	70.5 (6.0)	73.0 (5.5)	0.063
Mean (SD)				

CIS, clinically isolated syndrome; DMF, dimethyl fumarate; EDSS, Expanded Disability Status Scale; GA, glatiramer acetate; GCIPL, combined macular ganglion cell and inner plexiform layer; IFN, interferons; IQR, interquartile range; *N*, number; NT, Natalizumab; OR, optic radiation; ORL⁺, presence of new or enlarging optic radiation lesion at maximum follow-up; ORL⁻, absence of new or enlarging optic radiation lesion at maximum follow-up; pRNFL, peri-papillary retinal nerve fiber layer; RRMS, relapsing–remitting multiple sclerosis; SD, standard deviation.

¹Only non-ON eyes were included in the table.

0.13 ± 1.39 μm in ORL⁻ participants. Mean pRNFL decrease from baseline to 3-year follow-up was 1.27 ± 3.12 μm and 1.07 ± 3.20 μm in ORL⁺ and ORL⁻ participants, respectively. When comparing both groups in one model, the total GCIPL change in the eyes of the ORL⁺ participants at 3-year follow-up was more profound than those within the ORL⁻ group (total difference: -0.82 μm [95% CI: -1.49 to -0.15], *p* = 0.018). However, total pRNFL thinning did not differ between the two groups (total difference: -0.21 μm [95% CI: -1.43 to 1.01], *p* = 0.698). Considering there were more pweMS in the ORL⁺ group who had received DMT before study inclusion, we conducted a subgroup analysis excluding those who were on DMT treatment at baseline

to reduce the impact of treatment effects (Table S2). Compared to the ORL⁻ group, more profound GCIPL thinning was still observed in the ORL⁺ group.

Furthermore, we performed longitudinal analyses to explore the relationship between rates of GCIPL and pRNFL thinning with OR lesion volume change. A progressively increasing rate of GCIPL thinning was detected with enlarging OR lesion volume (β [95% CI] = -0.27 [-0.50 to -0.03], *p* = 0.028). No clear relationship was observed with pRNFL thinning (β [95% CI] = -0.02 [-0.18 to 0.14], *p* = 0.787) (Fig. 3). The effect size does not statistically differ between those with or without DMT treatments throughout the study period (Table S3). Similar correlations were detected when taking the

Table 2. Course of retinal layer thinning after 3-year follow-up.

	ORL ⁺	ORL ⁻	ORL ⁺ vs. ORL ⁻	
	Annualized thinning in retinal layer thickness, $\mu\text{m}/\text{year}$, mean (SD)	Annualized thinning in retinal layer thickness, $\mu\text{m}/\text{year}$, mean (SD)	Annualized thinning rate difference, $\mu\text{m}/\text{year}$, mean (SD)	Total change difference at 3rd year follow-up, μm , mean (SD)
GCIPL	-0.29 (0.06), $p = 3.34e^{-5}$	-0.12 (0.08), $p = 0.149$	-0.17 (0.11), $p = 0.134$	-0.82 (0.34), $p = 0.018$
pRNFL	-0.52 (0.22), $p = 0.026$	-0.38 (0.19), $p = 0.052$	-0.13 (0.33), $p = 0.707$	-0.21 (0.62), $p = 0.698$

GCIPL, combined macular ganglion cell and inner plexiform layer; ORL⁺, presence of new or enlarging optic radiation lesion at maximum follow-up; ORL⁻, absence of new or enlarging optic radiation lesion at maximum follow-up; pRNFL, peri-papillary retinal nerve fiber layer; SD, standard deviation.

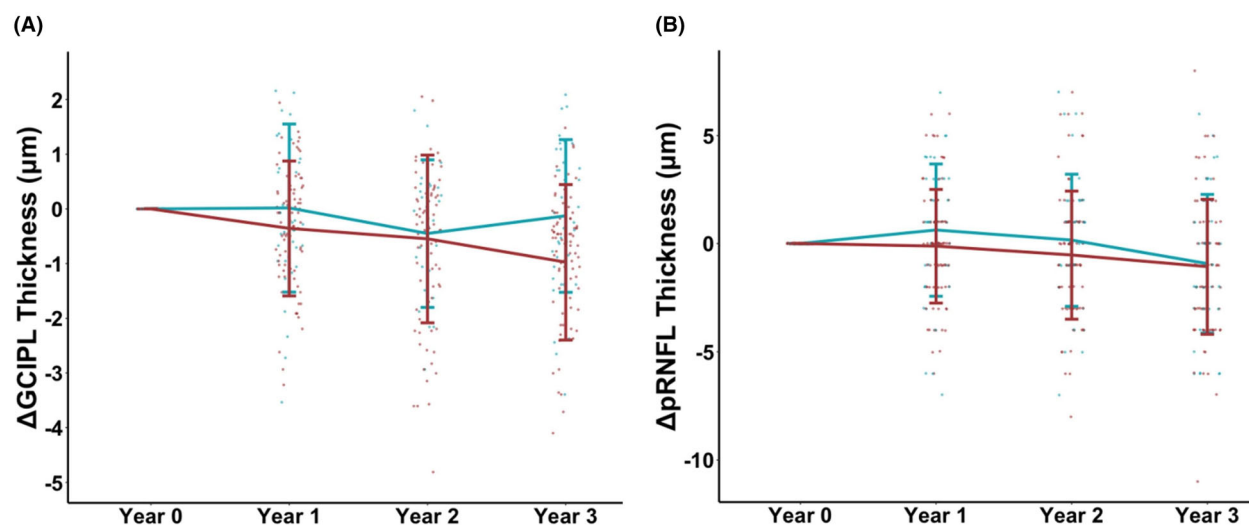


Figure 2. Changes of retinal layer thickness over time. Change of (A) GCIPL and (B) pRNFL in eyes of pweMS from the ORL⁺ (red) and the ORL⁻ (blue) groups over rounded time since baseline. GCIPL, combined macular ganglion cell and inner plexiform layer; ORL⁺, presence of new or enlarging optic radiation lesion at maximum follow-up; ORL⁻, absence of new or enlarging optic radiation lesion at maximum follow-up; pRNFL, peri-papillary retinal nerve fiber layer; pweMS, people with early multiple sclerosis.

changes in retinal layer thickness and OR lesion volume as annualized data (GCIPL: β [95% CI] = -0.31 [-0.55 to -0.06], $p = 0.019$; pRNFL: β [95% CI] = -0.09 [-0.31 to 0.10], $p = 0.323$).

Associations of OR lesion volume with homonymous hemi-macular GCIPL thinning

To identify further evidence of trans-synaptic neurodegeneration, we examined the relationship between unilateral optic radiation lesion volume and GCIPL thickness in the ipsilateral eyes, as well as homonymous hemi-macular GCIPL thinning (temporal quadrant of the ipsilateral eye [ipsi-T] and nasal quadrant of the contralateral eye [contra-N]).

At baseline, the unilateral OR lesion volume inversely correlated with GCIPL thickness of the ipsilateral eye (β

[95% CI] = -0.20 [-0.36 to -0.05], $p = 0.012$). Unilateral OR lesion volume was also associated with both ipsi-T GCIPL (β [95% CI] = -0.21 [-0.38 to -0.04], $p = 0.015$) and contra-N GCIPL (β [95% CI] = -0.21 [-0.38 to -0.03], $p = 0.018$). In terms of the counter hypothesis, we did not detect a correlation between higher unilateral OR lesion volume and lower contra-T GCIPL (β [95% CI] = -0.04 [-0.21 to 0.13], $p = 0.649$), but we did find a correlation with lower ipsi-N GCIPL (β [95% CI] = -0.17 [-0.34 to -0.01], $p = 0.031$).

Longitudinally, pweMS with increasing OR lesion volume showed ipsilateral GCIPL thinning (-0.26 [-0.43 to -0.09], $p = 0.004$), as well as ipsi-T GCIPL thinning (β [95% CI] = -0.21 [-0.40 to -0.02], $p = 0.030$) at 3-year follow-up. There was no association with contra-N GCIPL thinning (β [95% CI] = -0.05 [-0.23 to 0.13], $p = 0.604$), nor between unilateral OR lesion volume enlargement and either

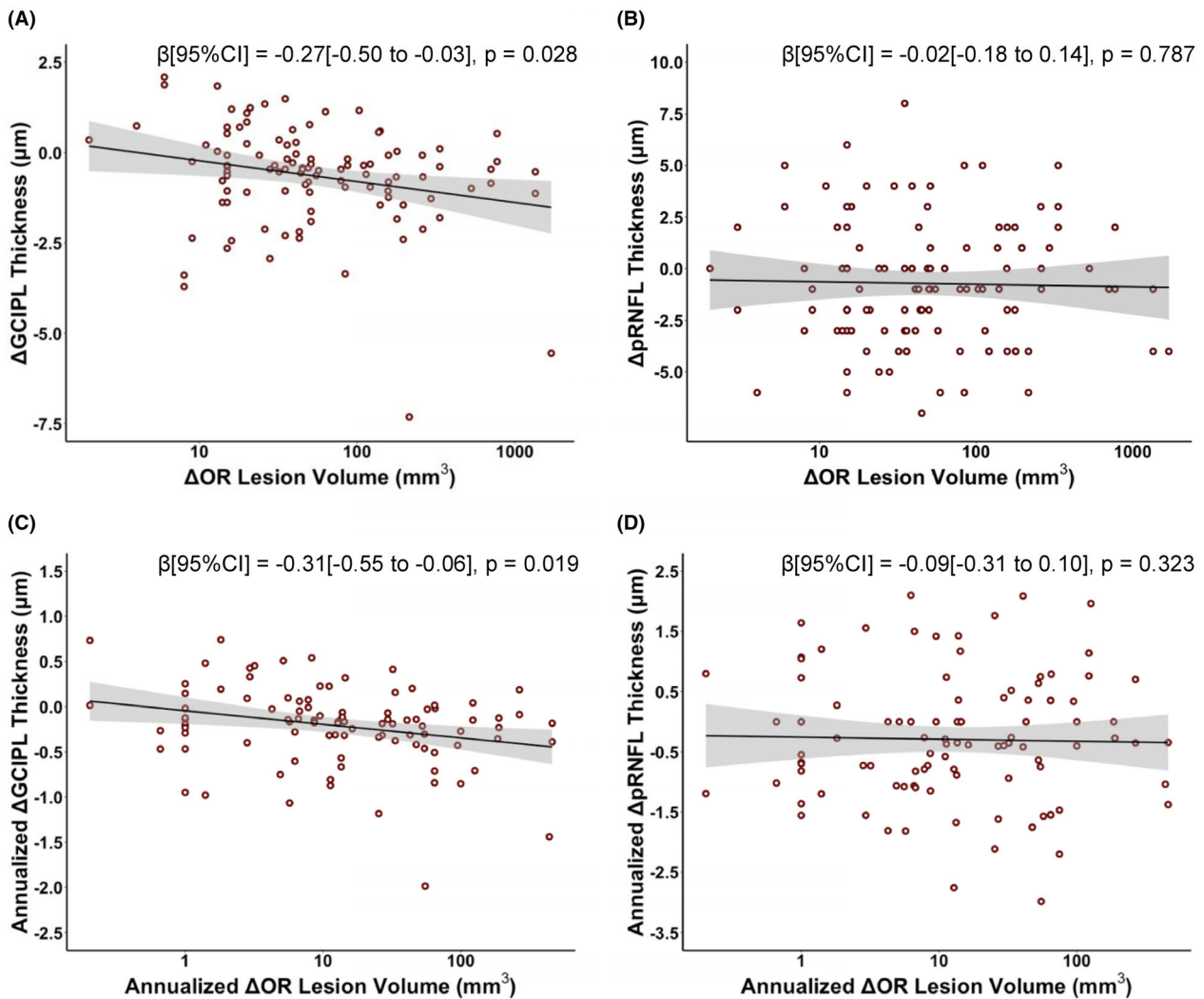


Figure 3. Longitudinal association of retinal layer thickness change with OR lesion volume change at 3-year follow-up. Scatterplots showing longitudinal correlation between total Δ OR lesion volume with (A) Δ GCIPL thickness and (B) Δ pRNFL thickness, and annualized Δ OR lesion volume with (C) annualized Δ GCIPL thickness and (D) annualized Δ pRNFL thickness at maximum follow-up. GCIPL, combined macular ganglion cell and inner plexiform layer; OR, optic radiation; pRNFL, peri-papillary retinal nerve fiber layer; SE, standard error; β , standardized estimate.

contralateral GCIPL (β [95% CI] = -0.12 [-0.30 to 0.06], $p = 0.175$) or heteronymous hemi-macular GCIPL thinning (contra-T: β [95% CI] = -0.18 [-0.36 to 0.01], $p = 0.052$; ipsi-N: β [95% CI] = -0.09 [-0.28 to 0.09], $p = 0.330$).

Longitudinal associations of retinal layer thinning with percentage of brain volume change

After a 3-year follow-up, the mean PBVC compared to baseline was $-1.02\% \pm 0.51\%$ ($p < 0.001$). In the analyses of retinal layer thinning with PBVC during follow-up, we found that PBVC was associated with changes in GCIPL thickness (β [95% CI] = 0.47 [0.25 to 0.70],

$p < 0.001$), but not with pRNFL (β [95% CI] = 0.03 [-0.18 to 0.23], $p = 0.808$). The same conclusion can also be drawn from the annualized data (results not shown).

Lastly, to evaluate whether the association between PBVC and GCIPL thinning was more evident in pweMS developing new or enlarging OR lesions, we conducted subgroup analyses between ORL^+ and the ORL^- group. pweMS in both groups showed a significant association between GCIPL thinning and PBVC, and interaction analyses showed no significant inter-group differences (ORL^+ : β [95% CI] = 0.50 [0.18 to 0.82], $p = 0.004$, ORL^- : β [95% CI] = 0.46 [0.13 to 0.79], $p = 0.029$; interaction effect: $\eta_p^2 = 5.92e^{-4}$, $p = 0.762$) (Table 3). The

Table 3. Association of changes in retinal layer thickness with changes in brain volumes in subgroups of pweMS with and without new OR lesions at 3-year follow-up.

	ORL ⁺	ORL ⁻
ΔGCIPL thickness ~ PBVC		
β (95%CI)	0.50 (0.18 to 0.82)	0.46 (0.13 to 0.79)
<i>p</i> -value	0.004	0.029
η_p^2 for interaction with PBVC, <i>p</i> -value	$\eta_p^2 = 5.92e^{-4}$, <i>p</i> = 0.762	
ΔpRNFL thickness ~ PBVC		
β (95%CI)	-0.09 (-0.39 to 0.21)	0.24 (-0.13 to 0.61)
<i>p</i> -value	0.947	0.204
η_p^2 for interaction with PBVC, <i>p</i> -value	$\eta_p^2 = 0.03$, <i>p</i> = 0.151	

CI, confidence interval; GCIPL, combined macular ganglion cell and inner plexiform layer; ORL⁺, presence of new or enlarging optic radiation lesion at maximum follow-up; ORL⁻, absence of new or enlarging optic radiation lesion at maximum follow-up; PBVC, percentage of brain volume change; pRNFL, peri-papillary retinal nerve fiber layer; pweMS, people with early multiple sclerosis; β , standardized estimate; η_p^2 , partial eta-squared.

association of pRNFL thinning with PBVC was still not detectable in either group (Table 3).

Discussion

In the present study, we investigated longitudinal quantitative changes of the RGC neuroaxonal damage in non-ON eyes and their relationships with inflammatory lesions localized within the OR regions in CIS and early MS. Our results suggest that pweMS with new or enlarging OR lesions had more progressive RGC neuroaxonal loss compared to those without. Moreover, changes in OR lesion volume and PBVC were associated with changes in GCIPL but not with pRNFL thickness over time.

The clinical value and pathophysiological mechanisms for RGC loss in non-ON eyes are under debate. Retrograde trans-synaptic degeneration theory has been suggested previously as a potential causal mechanism contributing to subclinical retinal neuroaxonal degeneration.^{9,11,12} The effects of this pathway-specific connection between progressive RGC degeneration and OR lesions have been demonstrated in cross-sectional and longitudinal studies that combined OCT and MRI investigations in long-standing RRMS.^{11,12,30,31} However, very few studies have investigated this hypothesis in CIS or early MS disease stages.¹³

In a prior study, using the same atlas-based OR lesion detection approach and targeting pweMS as in our study, a correlation between pRNFL and GCIPL thickness and OR lesion volume was only observed in 10 pweMS with

ON but not in 40 pweMS without ON.¹³ Therefore, it was suggested that ON might be a compulsory prerequisite for trans-synaptic degeneration of OR lesions, arguing against ON-independent mechanisms within the complex pathological process occurring in the visual pathway. However, the effect of RGC damage could solely be contributed by ON and not from the posterior visual pathway. Additionally, this study was limited by its purely cross-sectional design and its relatively small sample size. In contrast, our study only included eyes without a history of ON, and we discovered that pweMS with higher OR lesion load had thinner GCIPL and pRNFL. Nevertheless, the cross-sectional evidence cannot identify the causal relationship between first-order neurons and third-order neurons in the afferent visual pathway.

After a 3-year follow-up, the mean GCIPL and pRNFL thickness reduction from baseline in all pweMS was -0.70 ± 1.46 and -1.12 ± 3.14 μm , respectively. These results are comparable to the changes reported in the OCTiMS study, which included 333 pwMS with a mean time since MS diagnosis of 7.28 ± 5.75 years (-0.39 ± 3.10 and -1.61 ± 4.60 μm for GCIPL and pRNFL thickness reduction over 3 years, respectively).⁷ When taking OR lesion activity into account, pweMS who later developed new or enlarging OR lesions had a thinner GCIPL and pRNFL at baseline and a higher rate of inner retinal layer thinning over 3-year follow-up than those without. Our observations are in agreement with a prior study reporting that a more prominent temporal pRNFL thinning can be detected in RRMS patients with new OR lesional activity.¹¹ These findings support the hypothesis that the insidious injury of the retina can be partially attributed to damage in the posterior visual pathway.

Assessing the dynamic of OCT measures and OR lesion volume, our data confirmed the association between the longitudinal changes of the two measures. Intriguingly, this finding is more robust for thinning of GCIPL than pRNFL. This result supports the notion that GCIPL thickness measures may be more reliable than pRNFL thickness measures to reflect CNS radiologic disease activity.¹⁵ For instance, even though we excluded eyes with history of ON, we cannot fully eliminate the possibility of subclinical ON, which can still have microstructural changes of the retina, particularly pRNFL swelling.³² The association between GCIPL thinning and enlarging OR lesion size seems to be weaker in the first year follow-up, leading us to hypothesize that the amount of retinal atrophy in the early disease stage may not exceed the resolution limitation of the OCT device. Nevertheless, looking at the annualized changes, we still observed significant results.

Previous studies have described several cases of homonymous hemi-atrophy of the GCIPL in non-ON eyes

associated with posterior visual pathway inflammatory injuries involving OR, lateral geniculate nucleus or visual cortex.^{33–36} This relationship was observed not only in pwMS with homonymous hemianopia, but also in those with at least a certain degree of visual symptomatology. To further investigate this relationship and determine whether posterior visual pathway lesions showed good localizing features on retina atrophy, we also evaluated the correlation between homonymous hemi-macular GCIPL thinning and OR lesions. Our cross-sectional data showed an inverse correlation between unilateral OR lesion volume and both temporal GCIPL thickness in the ipsilateral eye and also the nasal GCIPL thickness in the contralateral eye. However, the longitudinal association of OR lesion volume enlargement with homonymous GCIPL hemi-atrophy was only significant with temporal GCIPL thinning on the ipsilateral side, but not with nasal GCIPL thinning on the contralateral side. We speculated that these unexpected findings may be due to possible influences of lesions in the contralateral OR. Nevertheless, excluding pweMS with a contralateral OR lesion during follow-up would have resulted in an insufficient sample size. On top of that, there were only a few cases with a link of homonymous hemi-macular thinning and inflammatory activities in the posterior visual pathway have been reported, suggesting that this may not be a universal finding in MS and requires larger studies with precise localization of retrochiasmatal lesions and exclude potential bilateral contribution to elucidate the causal relation. Lastly, a clear definition with sensitive thresholds for significant hemi-macular thinning is warranted. Mitchell *et al.*³⁷ suggested using the ipsi-lesional and contra-lesional GCIPL thickness difference with a normalized asymmetry score, whereas Mühlemann *et al.*³⁶ characterized it with a ratio lower than 0.9. A clear definition with sensitive thresholds for significant hemi-macular thinning is warranted.

Studies have shown cross-sectional and longitudinal relationships between OCT measures and brain atrophy previously.^{15,38–42} Our data confirmed and demonstrated clear evidence of retinal layer thinning correlates with decreasing PBVC also in pweMS. In accordance with previous studies, the association between brain atrophy and retinal layer thinning was more prominent in GCIPL than in pRNFL.^{15,43} This can be also explained by the confounding effect from potential subclinical micro-inflammation. Although we exclusively selected eyes without ON history at baseline and without ON attacks during follow-up, the possibility of subclinical optic disc swelling cannot be eliminated, hindering the interpretability of pRNFL thinning.

In a study of 161 pwMS, Pulido-Valdeolivas *et al.* reported that GCIPL thinning and whole-brain atrophy

were more prominent in the first 5 years after disease onset, particularly in those with focal inflammatory activity.⁴³ Furthermore, the recent OCTIMS study, including 333 pwMS, also described an association between percentage change of brain volume and change in GCIPL thickness over 3 years.⁷ Therefore, we further analyzed the contribution of focal lesion activity on the association between retinal atrophy and brain atrophy. When looking at the difference of OR lesion activity state, pweMS with and without new lesion in the OR region both showed a correlation between brain and retinal atrophy. This finding suggests that tract-specific association and global neurodegeneration may be two different pathophysiological concepts, one with inflammatory and the other with degenerative components. When evaluating brain atrophy measures, we always have to eliminate the possibility of pseudo-atrophy, a temporary decrease in brain volume due to inflammation and swelling that does not reflect an actual brain tissue loss.^{44,45} Our study had multiple follow-ups to confirm the occurrence of significant brain volume change.

We are aware of several limitations of our study. Despite having a well-characterized cohort, one fundamental limitation arises from the monocentric and homogenous study design. Additionally, with a limited sample size of participants without OR lesions at study inclusion, we could not compare the course of retinal atrophy in those pweMS with the ones who already featured OR lesions at baseline. This also refrains us from analyzing the impact of lesions outside the OR regions. Future studies with a larger sample size and longer follow-up under multicenter settings could corroborate the validity of our findings. Furthermore, pweMS within the ORL⁺ group have a higher rate of DMT treatment compared to ORL⁻ group, suggesting to be a potential confounder. Even though further subgroup analyses showed no significant difference between those with or without treatment, the difference of treatment status should still be taken into account when interpreting the results. Lastly, there is no gold standard for OR lesion *in vivo* assessment, causing the validity of OR lesions reported herein to be limited regarding its true informative value. Without a consensus on the definition of new OR lesion activity, the threshold used in the study is arbitrary. However, atlas template-based approaches, as it was used in our study, are particularly suited to the semi-automated analysis of large image datasets. They provide equivalent informative value on lesion quantification compared to other advanced MRI approaches to delineate the ORs, such as diffusion-weighted MR probabilistic tractography.⁴⁶

In conclusion, our study demonstrated more pronounced pRNFL and GCIPL loss in pweMS with an

increase in OR lesions compared to those with stable OR lesions. The extent of the increase in OR lesion volume also correlated with the rate of RGC neuroaxonal damage, as well as homonymous hemi-macular GCIPL thinning. Furthermore, whole-brain atrophy is associated with sub-clinical neuroaxonal damage in the retina over time, independent of new or enlarging OR lesions. Future large multi-centered studies with regular interval longitudinal OCT and MRI investigations are highly warranted to establish more concrete evidence regarding the relationship between RGC loss and OR lesion activity throughout the MS disease course. Additionally, detailed analyses on OR lesion enlarging rate and the impact of newly emerging OR lesions over time in association with OCT retinal changes could elucidate the time course of trans-synaptic neuropathological processes between posterior visual pathway inflammatory lesions and retinal pathology in MS.

Author Contributions

Ting-Yi Lin collected and curated the data; implemented the method; performed the analyses; and drafted the manuscript for intellectual content. Claudia Chien designed and implemented the method; and revised the manuscript for intellectual content. Joseph Kuchling designed and implemented the method; and revised the manuscript for intellectual content. Susanna Asseyer contributed to data collection; and revised the manuscript for intellectual content. Seyedamirhossein Motamedi contributed to the method implementation; and revised the manuscript for intellectual content. Judith Bellmann-Strobl contributed to data collection; and revised the manuscript for intellectual content. Tanja Schmitz-Hübisch contributed to data collection; and revised the manuscript for intellectual content. Klemens Ruprecht contributed to data collection; and revised the manuscript for intellectual content. Alexander U. Brandt contributed to data interpretation; and revised the manuscript for intellectual content. Hanna G. Zimmermann designed and conceptualized the study; contributed to study management; and revised the manuscript for intellectual content. Friedemann Paul designed and conceptualized the study; contributed to study management; and revised the manuscript for intellectual content.

Acknowledgements

We thank Charlotte Bereuter, Carla Leutloff, Susan Pikol, and Cynthia Kraut for their excellent assistance with OCT and MRI, respectively. Open Access funding enabled and organized by Projekt DEAL.

Funding Information

The study was supported by a limited research grant from Bayer Vital GmbH (to FP).

Conflict of Interest

T.-Y. Lin has received compensation from ADA Health, unrelated to the presented work. C. Chien has received research support from Novartis and Alexion and speaking and writing honoraria from Bayer Healthcare and the British Society for Immunology, as well as serves as a member of the Standing Committee on Science for the Canadian Institutes of Health Research (CIHR). J. Kuchling has received congress registration fees from Biogen, and speaker honoraria from Sanofi Genzyme and Bayer Schering. JK is participant in the BIH-Charité Junior Clinician Scientist Program funded by the Charité—Universitätsmedizin Berlin and Berlin Institute of Health. S. Asseyer has received speaking honoraria from Alexion, Bayer, and Roche. S. Motamedi reports no relevant disclosures. J. Bellmann-Strobl has received travel grants and speaking honoraria from Bayer Healthcare, Biogen Idec, Merck Serono, Sanofi Genzyme, Teva Pharmaceuticals, Roche, and Novartis, none of them related to this work. T. Schmitz-Hübisch reports no relevant disclosures. K. Ruprecht received research support from Novartis, Merck Serono, German Ministry of Education and Research, European Union (821283-2), Stiftung Charité, Guthy-Jackson Charitable Foundation, and Arthur Arnstein Foundation; received travel grants from Guthy-Jackson Charitable Foundation; received speaker's honoraria from Novartis. KR is a participant in the BIH Clinical Fellow Program funded by Stiftung Charité. A.U. Brandt is cofounder and holds shares of medical technology companies Motognosis GmbH and Nocturne GmbH. He is named as inventor on several patents and patent applications describing methods for retinal image analyses, motor function analysis, multiple sclerosis serum biomarkers and myelination therapies utilizing N-glycosylation modification. He is cofounder of IMSVISUAL. AUB is now full-time employee and holds stocks and stock options of Eli Lilly and Company. His contribution to this work is his own and does not represent a contribution from Eli Lilly. H.G. Zimmermann received research grants from Novartis and speaking honoraria from Novartis and Bayer Healthcare. F. Paul served on the scientific advisory boards of Novartis and MedImmune; received travel funding and/or speaker honoraria from Bayer, Novartis, Biogen, Teva, Sanofi-Aventis/Genzyme, Merck Serono, Alexion, Chugai, MedImmune, and Shire; is an associate editor of *Neurology: Neuroimmunology & Neuroinflammation*; is an academic editor of *PLoS ONE*; consulted for Sanofi

Genzyme, Biogen, MedImmune, Shire, and Alexion; received research support from Bayer, Novartis, Biogen, Teva, Sanofi-Aventis/Genzyme, Alexion, and Merck Serono; and received research support from the German Research Council, Werth Stiftung of the City of Cologne, German Ministry of Education and Research, Arthur Arnstein Stiftung Berlin, EU FP7 Framework Program, Arthur Arnstein Foundation Berlin, Guthy-Jackson Charitable Foundation, and NMSS.

References

- Reich DS, Lucchinetti CF, Calabresi PA. Multiple Sclerosis. *N Engl J Med*. 2018;378:169-180.
- Balcer LJ, Miller DH, Reingold SC, Cohen JA. Vision and vision-related outcome measures in multiple sclerosis. *Brain*. 2015;138:11-27.
- Graves JS, Oertel FC, Van der Walt A, et al. Leveraging visual outcome measures to advance therapy development in neuroimmunologic disorders. *Neurol Neuroimmunol Neuroinflamm*. 2022;9:e1126.
- Kuchling J, Paul F. Visualizing the central nervous system: imaging tools for multiple sclerosis and neuromyelitis Optica Spectrum disorders. *Front Neurol*. 2020;11:1-21.
- Petzold A, Fraser CL, Abegg M, et al. Diagnosis and classification of optic neuritis. *Lancet Neurol*. 2022;21:1120-1134.
- Petzold A, Balcer L, Calabresi PA, et al. Retinal layer segmentation in multiple sclerosis: a systematic review and meta-analysis. *Lancet Neurol*. 2017;16:797-812.
- Paul F, Calabresi PA, Barkhof F, et al. Optical coherence tomography in multiple sclerosis: a 3-year prospective multicenter study. *Ann Clin Transl Neurol*. 2021;8:2235-2251.
- Green AJ, McQuaid S, Hauser SL, Allen IV, Lyness R. Ocular pathology in multiple sclerosis: retinal atrophy and inflammation irrespective of disease duration. *Brain*. 2010;133:1591-1601.
- Balk LJ, Steenwijk MD, Tewarie P, et al. Bidirectional trans-synaptic axonal degeneration in the visual pathway in multiple sclerosis. *J Neurol Neurosurg Psychiatry*. 2015;86:419-424.
- Tur C, Goodkin O, Altmann DR, et al. Longitudinal evidence for anterograde trans-synaptic degeneration after optic neuritis. *Brain*. 2016;139:816-828.
- Klistorner A, Graham EC, Yiannikas C, et al. Progression of retinal ganglion cell loss in multiple sclerosis is associated with new lesions in the optic radiations. *Eur J Neurol*. 2017;24:1392-1398.
- Sinnecker T, Oberwahrenbrock T, Metz I, et al. Optic radiation damage in multiple sclerosis is associated with visual dysfunction and retinal thinning – an ultrahigh-field MR pilot study. *Eur Radiol*. 2015;25:122-131.
- Puthenparampil M, Federle L, Poggiali D, et al. Trans-synaptic degeneration in the optic pathway. A study in clinically isolated syndrome and early relapsing-remitting multiple sclerosis with or without optic neuritis. *PLoS One*. 2017;12:e0183957.
- Borgström M, Tisell A, Link H, Wilhelm E, Lundberg P, Huang-Link Y. Retinal thinning and brain atrophy in early MS and CIS. *Acta Neurol Scand*. 2020;142:418-427.
- Saidha S, Al-Louzi O, Ratchford JN, et al. Optical coherence tomography reflects brain atrophy in multiple sclerosis: a four-year study. *Ann Neurol*. 2015;78:801-813.
- Sotirchos ES, Saidha S. OCT is an alternative to MRI for monitoring MS – YES. *Mult Scler J*. 2018;24:701-703.
- Brandt AU, Martinez-Lapiscina EH, Nolan R, Saidha S. Monitoring the course of MS with optical coherence tomography. *Curr Treat Options Neurol*. 2017;19:19.
- Thompson AJ, Banwell BL, Barkhof F, et al. Diagnosis of multiple sclerosis: 2017 revisions of the McDonald criteria. *Lancet Neurol*. 2018;17:162-173.
- Motamedi S, Gawlik K, Ayadi N, et al. Normative data and minimally detectable change for inner retinal layer thicknesses using a semi-automated OCT image segmentation pipeline. *Front Neurol*. 2019;10:1117.
- Lin T-Y, Vitkova V, Assejer S, et al. Increased serum neurofilament light and thin ganglion cell-inner plexiform layer are additive risk factors for disease activity in early MS. *Neurol Neuroimmunol Neuroinflamm*. 2021;8:e1051.
- Cruz-Herranz A, Balk LJ, Oberwahrenbrock T, et al. The APOSTEL recommendations for reporting quantitative optical coherence tomography studies. *Neurology*. 2016;86:2303-2309.
- Schippling S, Balk LJ, Costello F, et al. Quality control for retinal OCT in multiple sclerosis: validation of the OSCAR-IB criteria. *Mult Scler J*. 2015;21:163-170.
- Smith SM, Jenkinson M, Woolrich MW, et al. Advances in functional and structural MR image analysis and implementation as FSL. *Neuroimage*. 2004;23:208-219.
- Yushkevich PA, Piven J, Hazlett HC, et al. User-guided 3D active contour segmentation of anatomical structures: significantly improved efficiency and reliability. *Neuroimage*. 2006;31:1116-1128.
- Battaglini M, Jenkinson M, De Stefano N. Evaluating and reducing the impact of white matter lesions on brain volume measurements. *Hum Brain Mapp*. 2012;33:2062-2071.
- Bürgel U, Schormann T, Schleicher A, Zilles K. Mapping of histologically identified long fiber tracts in human cerebral hemispheres to the MRI volume of a reference brain: position and spatial variability of the optic radiation. *Neuroimage*. 1999;10:489-499.
- Smith SM, Zhang Y, Jenkinson M, et al. Accurate, robust, and automated longitudinal and cross-sectional brain change analysis. *Neuroimage*. 2002;17:479-489.

28. Ge Y. Multiple sclerosis: the role of MR imaging. *Am J Neuroradiol.* 2006;27:1165-1176.
29. R Core Team. R: A language and environment for statistical computing. R Foundation for Statistical Computing; 2018.
30. Gabilondo I, Martínez-Lapiscina EH, Martínez-Heras E, et al. Trans-synaptic axonal degeneration in the visual pathway in multiple sclerosis. *Ann Neurol.* 2014;75:98-107.
31. Klistorner A, Sriram P, Vootakuru N, et al. Axonal loss of retinal neurons in multiple sclerosis associated with optic radiation lesions. *Neurology.* 2014;82:2165-2172.
32. Costello F, Pan YI, Yeh EA, Hodge W, Burton JM, Kardon R. The temporal evolution of structural and functional measures after acute optic neuritis. *J Neurol Neurosurg Psychiatry.* 2015;86:1369-1373.
33. Oh J, Sotirchos ES, Saidha S, et al. In vivo demonstration of homonymous Hemimacular loss of retinal ganglion cells due to a thalamic lesion using optical coherence tomography. *JAMA Neurol.* 2013;70:410-411.
34. Al-Louzi O, Button J, Newsome SD, Calabresi PA, Saidha S. Retrograde trans-synaptic visual pathway degeneration in multiple sclerosis: a case series. *Mult Scler.* 2017;23:1035-1039.
35. Lukewich MK, Schlenker MB, Micieli JA. Homonymous hemi-macular atrophy of the ganglion cell-inner plexiform layer with preserved visual function. *J Neurol Sci Elsevier.* 2020;417:117072.
36. Mühlemann F, Grabe H, Fok A, et al. Homonymous hemiatrophy of ganglion cell layer from retrochiasmatal lesions in the visual pathway. *Neurology.* 2020;94:e323-e329.
37. Mitchell JR, Oliveira C, Tsiouris AJ, Dinkin MJ. Corresponding ganglion cell atrophy in patients with Postgeniculate homonymous visual field loss. *J Neuro-Ophthalmology.* 2015;35:353-359.
38. Gordon-Lipkin E, Chodkowski B, Reich DS, et al. Retinal nerve fiber layer is associated with brain atrophy in multiple sclerosis: reply. *Neurology.* 2008;69:1603-1609.
39. Siger M, Dzi gielewski K, Jasek L, et al. Optical coherence tomography in multiple sclerosis: thickness of the retinal nerve fiber layer as a potential measure of axonal loss and brain atrophy. *J Neurol.* 2008;255:1555-1560.
40. Dörr J, Wernecke KD, Bock M, et al. Association of retinal and macular damage with brain atrophy in multiple sclerosis. *PloS One.* 2011;6:2-7.
41. Young KL, Brandt AU, Petzold A, et al. Loss of retinal nerve fibre layer axons indicates white but not grey matter damage in early multiple sclerosis. *Eur J Neurol.* 2013;20:803-811.
42. Frau J, Fenu G, Signori A, et al. A cross-sectional and longitudinal study evaluating brain volumes, RNFL, and cognitive functions in MS patients and healthy controls. *BMC neurol. BMC Neurol.* 2018;18:67.
43. Pulido-Valdeolivas I, Andorrà M, Gómez-Andrés D, et al. Retinal and brain damage during multiple sclerosis course: inflammatory activity is a key factor in the first 5 years. *Sci Rep.* 2020;10:13333.
44. De Stefano N, Airas L, Grigoriadis N, et al. Clinical relevance of brain volume measures in multiple sclerosis. *CNS Drugs.* 2014;28:147-156.
45. De Stefano N, Giorgio A, Gentile G, et al. Dynamics of pseudo-atrophy in RRMS reveals predominant gray matter compartmentalization. *Ann Clin Transl Neurol.* 2021;8:623-630.
46. Kuchling J, Backner Y, Oertel FC, et al. Comparison of probabilistic tractography and tract-based spatial statistics for assessing optic radiation damage in patients with autoimmune inflammatory disorders of the central nervous system. *NeuroImage Clin.* 2018;19:538-550.

Supporting Information

Additional supporting information may be found online in the Supporting Information section at the end of the article.

Tables S1–S3